

Extending LLMs’ Context Window with 100 Samples

Anonymous ACL submission

Abstract

Large Language Models (LLMs) are known to have limited extrapolation ability beyond their pre-trained context window, constraining their application in downstream tasks with lengthy inputs. Recent studies have sought to extend LLMs’ context window by modifying rotary position embedding (RoPE), a popular position encoding method adopted by well-known LLMs such as LLaMA, PaLM, and GPT-NeoX. However, prior works like Position Interpolation (PI) and YaRN are resource-intensive and lack comprehensive experiments to assess their applicability. In this work, we identify the inherent need for LLMs’ attention entropy (i.e. the information entropy of attention scores) to maintain stability and introduce a novel extension to RoPE which combines adjusting RoPE’s base frequency and scaling the attention logits to help LLMs efficiently adapt to a larger context window. We validate the superiority of our method in both fine-tuning performance and robustness across different context window sizes on various context-demanding tasks. Notably, our method extends the context window of LLaMA-2-7B-Chat to 16,384 with only 100 samples and 6 training steps, showcasing extraordinary efficiency. Finally, we also explore how data compositions and training curricula affect context window extension for specific downstream tasks, suggesting fine-tuning LLMs with lengthy conversations as a good starting point. We release our code and SFT data at <https://anonymous.4open.science/r/Entropy-ABF-0084/README.md>.

1 Introduction

Large Language Models (LLMs) are typically pre-trained with a pre-defined context window size. For instance, LLaMA 2 (Touvron et al., 2023b) is pre-trained on sequences of 4,096 tokens. When exceeding the pre-trained context window, the performance of LLMs tends to deteriorate primarily due to the limited length extrapolation ability of their

position encoding methods (Kazemnejad et al., 2023). The limited context window affects LLMs’ practicality for ever-increasing context-demanding tasks such as few-shot learning (Brown et al., 2020), long document summarization (Huang et al., 2021) and repository-level code completion (Liu et al., 2023). Consequently, there is an urgent need to extend LLMs’ context window.

To meet this pressing demand, recent works have witnessed progress in context window extension in both fine-tuned and non-fine-tuned scenarios by extending Rotary Position Embedding (RoPE) (Su et al., 2021), a widely-used position encoding method adopted by state-of-the-art LLMs such as LLaMA (Touvron et al., 2023a,b), PaLM (Chowdhery et al., 2023; Anil et al., 2023) and GPT-NeoX (Black et al., 2022). For example, Position Interpolation (PI) (kaiokendev, 2023; Chen et al., 2023) linearly down-scales the input tokens’ position indices and achieves improved fine-tuning results. NTK-Aware scaling (bloc97, 2023b) and adjusted base frequency (ABF) (Xiong et al., 2023) modify the base frequency of RoPE, leading to enhanced results in fine-tuning and non-fine-tuning scenarios respectively. NTK-By-Parts scaling (bloc97, 2023a) treats different dimensions differently and reports even better fine-tuning outcomes. More recently, YaRN (Peng et al., 2023) proposes scaling the attention logits given its beneficial effects on language modeling perplexity. They combine this scaling technique with NTK-By-Parts scaling and report the best long-context performance among existing RoPE-extension methods.

However, the underlying rationale behind the efficiency of the scaling operation in YaRN, which results in the best-reported context window extension performance, remains poorly understood. In this study, we first provide an interpretation of this technique by analyzing its effect on stabilizing the information entropy of models’ attention

scores and then introduce our own RoPE-extension method termed “entropy-aware ABF”, which combines ABF with a sophisticated utilization of dynamic attention scalar.

Moreover, despite the *individual-reported* efficacy of previous RoPE-extension methods, there’s a lack of comprehensive *comparative* analysis where different methods are put in the same evaluation testbed. This study also addresses this gap by answering three key questions pertinent to context window extension in real-world applications: (1) Which method exhibits the best supervised fine-tuning performance on context-demanding downstream tasks? (2) How can each method efficiently utilize training data? (3) Do models trained with these methods have a robust performance across varying context window sizes?

To answer the above questions, we conduct experiments on a diverse set of context-demanding tasks from LongBench (Bai et al., 2023), manipulating the training data amounts and prompt lengths to evaluate fine-tuned models across different dimensions. The experiment results demonstrate that models trained with our method surpass all baselines in long-context fine-tuning performance and also maintain a robust performance across various context window sizes. Notably, with only 100 long conversations from ShareGPT (Chiang et al., 2023) and 6 training steps, using four A100 GPUs for approximately 6 minutes, our method produces a model with competent performance across 12 selected context-demanding tasks. Finally, we explore the influence of data compositions and training curricula on context window extension for a given long context downstream task, suggesting fine-tuning the model on lengthy ShareGPT conversations as a good starting point.

2 Preliminaries

Rotary Position Embedding (RoPE) Given a position index $m \in [1, c]$ and an embedding vector $\mathbf{x} := [x_0, x_1, \dots, x_{d-1}]^\top$, where d is the dimension of each attention head, RoPE considers each pair of elements along the feature dimension of the embedding vector as complex numbers and encodes position information by rotating them. The vector-valued complex function $\mathbf{f}(\mathbf{x}, m)$ defined by RoPE is as follows:

$$\mathbf{f}(\mathbf{x}, m) = \begin{bmatrix} (x_0 + ix_1)e^{im\theta_1}, \\ (x_2 + ix_3)e^{im\theta_2}, \\ \dots, \\ (x_{d-2} + ix_{d-1})e^{im\theta_{d/2}} \end{bmatrix} \quad (1)$$

$i := \sqrt{-1}$ is the imaginary unit and $\theta_j = b^{-2j/d}$, where b denotes the base frequency of RoPE and is set to 10,000 by default.

In application, RoPE is applied to both query and key embeddings through the following equation:

$$\mathbf{f}(\mathbf{x}, m) = \begin{bmatrix} x_0 \\ x_1 \\ x_2 \\ x_3 \\ \vdots \\ x_{d-2} \\ x_{d-1} \end{bmatrix} \otimes \begin{bmatrix} \cos(m\theta_0) \\ \cos(m\theta_0) \\ \cos(m\theta_1) \\ \cos(m\theta_1) \\ \vdots \\ \cos(m\theta_{(d-1)/2}) \\ \cos(m\theta_{(d-1)/2}) \end{bmatrix} + \begin{bmatrix} -x_1 \\ x_0 \\ -x_3 \\ x_2 \\ \vdots \\ -x_{d-1} \\ x_{d-2} \end{bmatrix} \otimes \begin{bmatrix} \sin(m\theta_0) \\ \sin(m\theta_0) \\ \sin(m\theta_1) \\ \sin(m\theta_1) \\ \vdots \\ \sin(m\theta_{(d-1)/2}) \\ \sin(m\theta_{(d-1)/2}) \end{bmatrix} \quad (2)$$

The fundamental components of RoPE are a series of trigonometric coefficients, each encoding position information of different frequencies.

We represent these trigonometric coefficients with the following function to uniquely identify RoPE and its variants:

$$h(m, b, t) = \sqrt{t} * \cos\left(\frac{m}{\frac{2j}{d}}\right) \text{ or } \sqrt{t} * \sin\left(\frac{m}{\frac{2j}{d}}\right) \quad (3)$$

where m is the position index of the query token, b is the base frequency for RoPE, and t is the scaling factor for attention logits. Note that \sqrt{t} is used in the equation because RoPE rotates process both the query and key embeddings.

Before introducing RoPE-extension methods that enable better context window extension, we define context scaling factor $s = \frac{c'}{c}$, which is the ratio between the target context window c' and the pre-trained context window c . It is of special use to those methods that extend RoPE according to a given target context window size.

Position Interpolation (PI) PI (Chen et al., 2023; kaiokendev, 2023) linearly interpolates the input position index m to $\frac{m}{s}$ so that it falls within the original context window size. Chen et al. (2023) demonstrate that direct fine-tuning of LLaMA (Touvron et al., 2023a) with an extended context window results in minimal improvement, as the effective context window of the model only increases from 2,048 to 2560 after 10,000 training steps on sequences of length 8,192. By contrast, PI succeeds in extending the context window of LLaMA to 32,768 with only 1,000 training steps.

NTK-Aware NTK-Aware scaling (bloc97, 2023b) hypothesize that interpolating all dimensions equally, as done by PI, may result in loss of high-frequency information. Therefore, NTK-Aware scaling introduces a nonlinear interpolation strategy by adjusting the base frequency b of RoPE to $b^{\frac{d}{d-2}}$. This modification scales the

low-frequency components of RoPE to a similar extent as PI, while only slightly altering the high-frequency components to avoid disturbing high-frequency information. NTK-Aware extends models’ context window size without training. However, this method can’t benefit as much as PI from additional training on longer sequences as suggested by (Peng et al., 2023).

NTK-By-Parts NTK-By-Parts (bloc97, 2023a) holds that stretching all the RoPE components either by a scaling factor s or a base transformation results in token embeddings being closer to each other, impeding LLMs from effectively capturing local relationships between adjacent tokens. To address this issue, NTK-By-Parts scales $\theta(j)$ by a factor $\frac{1-\gamma(j)}{s} + \gamma(j)$, with $\gamma(j)$ being assigned 0 for high frequencies, 1 for low frequencies, and a predetermined constant within the range of 0 to 1 for intermediate frequencies. According to (Peng et al., 2023), this method performs better than PI and NTK-Aware scaling for both fine-tuned and non-fine-tuned models.

YaRN Yarn (Peng et al., 2023) empirically observes that introducing a temperature t to scale the attention logits before the softmax function improves models’ language modeling performance. They find the optimal value of $\sqrt{t} = 0.1 \ln s + 1$ by fitting the lowest perplexity curve against various context scaling factors s . They combine their finding with NTK-By-Parts scaling and term this method YaRN (Yet another RoPE extension method). YaRN reports the best long-context performance on language modeling tasks among existing methods.

Adjusted Base Frequency (ABF) ABF (Xiong et al., 2023) simply changes the base frequency of RoPE to 50,000. Both theoretical analysis and experiment are conducted to validate the efficacy of this method. Xiong et al. (2023) proves that ABF minimizes the distance of its embedded vectors from the ones using the original RoPE, which helps leverage the pre-training results. They empirically validate the efficacy of ABF by showing a lower perplexity on language modeling tasks and a longer effective context window in the first-sentence-retrieval task.

Table 1 highlights the difference between RoPE and its variants by specifying the different m , b , and t they use in Equation 3 and whether they require additional training for context window extension:

Method	m	b	t	Additional Training
RoPE	m	10,000	1	-
PI	m/s	10,000	1	continual pre-train
NTK-Aware	m	$10,000 \frac{d-d^2}{d}$	1	-
NTK-By-Parts	$(\frac{1-\gamma(j)}{s} + \gamma(j))m$	10,000	1	continual pre-train
YaRN	$(\frac{1-\gamma(j)}{s} + \gamma(j))m$	10,000	$0.1 \ln(s) + 1$	continual pre-train
ABF	m	500,000	1	continual pre-train

Table 1: An overview of Rotary Position Embedding (RoPE) and its variants represented by Equation 3.

3 Proposal Method

YaRN (Peng et al., 2023) introduces a scaling factor t on the attention logits based on empirical evidence indicating its beneficial effects on language modeling perplexities. However, the underlying rationale behind this technique remains poorly understood. In this section, we first introduce an interpretation of this technique, which motivates our method.

3.1 Interpretation of YaRN’s Scaling Factor

In Transformer models’ attention mechanism (Vaswani et al., 2017), the Softmax function forces attention scores assigned to contextual tokens to sum to one while concurrently preventing any individual score from becoming zero. Consequently, with an increasing number of input tokens, LLMs will theoretically distribute more attention across more tokens and lead to a rise in what we refer to as “attention entropy”, which quantifies the randomness within the distribution of attention scores and is calculated using the following equation:

$$\text{attention_entropy} = \sum_i -p_i \ln p_i \quad (4)$$

where p_i is the attention scores assigned to contextual tokens.

To validate the aforementioned theoretical effect, we utilized LLaMA-2-7B-Chat (Touvron et al., 2023b) to process 128 randomly chosen documents from the Pile dataset (Gao et al., 2020). We collect the attention scores assigned to contextual tokens for query tokens at different input positions to simulate varying numbers of contextual tokens. Subsequently, we compute the information entropy for these attention scores on different model layers via Equation 4. The resulting average attention entropies over our randomly sampled documents are visualized in Figure 1.

Counterintuitively, only the first two model layers demonstrate a steady rise in attention entropy.

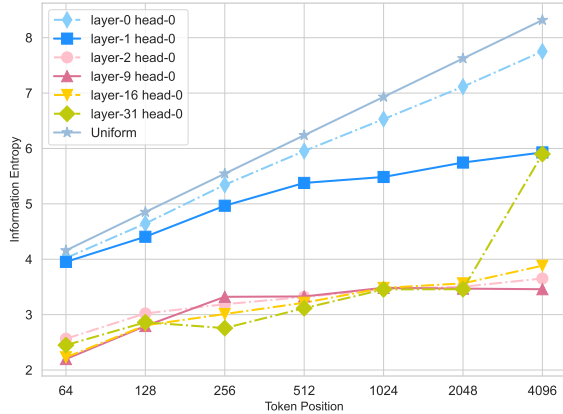


Figure 1: Visualization of the averaged attention entropy for query tokens at different input positions in the LLaMA-2-7B-chat model across the selected 128 documents from the Pile-arXiv dataset (Gao et al., 2020). “Uniform” represents a uniform attention score distribution, which corresponds to $\text{attention_entropy} = \ln n$ with n denoting the number of contextual tokens.

Interestingly, we even observe that the attention entropies of all the subsequent layers remain remarkably similar when the number of contextual tokens increases from 1,024 to 2,048.

This finding of LLMs maintaining a stable attention entropy in subsequent model layers leads us to posit that possessing a certain degree of length-invariance in attention entropy in these layers is an important inherent characteristic. When modeling longer sequences than encountered in the pre-training stage, LLMs might fail to concentrate well, leading to a performance drop. Thanks to the exponential function in Softmax, scaling the attention logits reduces attention entropy, thereby explaining why it leads to improvements in language modeling tasks when modeling lengthy inputs as observed in YaRN (Peng et al., 2023).

3.2 Design Principles

Previous works have explored different scaling factors on the attention logits with different motivations. Chiang and Cholak (2022) scales the attention logits by $\log n$, with n representing the length of the longest training sequence, to enhance the model’s extrapolation ability in downstream tasks such as machine translation.

More recently, YaRN (Peng et al., 2023) introduces the scaling factor $t = 0.1 \ln s + 1$ by fitting the lowest perplexity curve in language modeling tasks. They combine these scaling factors with NTK-By-Parts scaling and observe improved fine-

tuning long-context performance on language modeling tasks.

ReRoPE (Su, 2023) utilized a dynamic scaling factor that takes into account the number of contextual tokens for each input position: $t = \log_c m$, where c denotes the pre-trained context window size and m represents the position index of input tokens. By introducing this scaling factor during the pre-training stage, ReRoPE demonstrates enhanced extrapolation ability in language modeling tasks, which is also observed in YaRN.

We propose “entropy-aware ABF” with the following design principles:

(1). Dynamic Attention Scaling: Both PI and YaRN employ a *constant* scaling factor for all input positions, which may excessively stretch the attention logits at the front positions and hinder the model’s ability to extrapolate to longer sequences. Instead of using a constant scaling factor, we propose using a dynamic factor that takes into account the number of contextual tokens for each input position. This allows the model to adjust the attention weights more flexibly based on the level of randomness in the distribution of attention scores.

(2). Layer-dependent: All the existing works apply the scalar indiscriminately to all model layers. However, based on our observations in Figure 1 that the first two layers consistently exhibit a near-uniform attention pattern and only the latter layers demonstrate the tendency to maintain concentration, we propose not to intervene in the first two layers to align with the model’s inherent characteristics.

(3). Facilitate Context Window Extension: Furthermore, we hypothesize that learning to maintain concentration when processing lengthy sequences is critical to context window extension, and scaling the attention logits can serve as an inductive bias that facilitates this process. This motivates us to combine “scaling the attention logits” with ABF during the supervised fine-tuning stage. To leverage the pretraining results, we also propose the avoidance of modifying the attention logits within the pre-trained context window by setting a lower bound to t .

Our ultimate scaling factor t is depicted as below:

$$t = \begin{cases} 1, & \text{if layer index is 0 or 1} \\ \max(\log_c i, 1), & \text{o.w.} \end{cases}$$

4 Experiments

To analyze the real-world applicability of different RoPE-extension methods, we test the long-context performance of models trained with these methods on selected tasks from LongBench (Bai et al., 2023) and answer the three research questions we propose in Section 1 by adjusting training data amount and context window sizes. Finally, we also explore efficient data compositions and training curricula on context window extension for given downstream tasks.

4.1 General Setup

Model Variants We use LLaMA-2-7B-Chat (Touvron et al., 2023b) given its popularity. We only modify RoPE while leaving the model architecture unchanged.

Training Previous works (Chen et al., 2023; Xiong et al., 2023; Peng et al., 2023) adopt a similar training curriculum by first continual pre-training the LLaMA base model to adapt to the modified position embeddings and then fine-tune on target long-context downstream tasks. In contrast, we propose directly supervised fine-tuning of the Chat Model to evaluate the practical applicability of different RoPE-extension methods. We extend the context window of LLaMA-2-7B-Chat to 16k with detailed training setups available in Appendix A.

SFT Data We curate a dataset of 3.5k lengthy conversations from ShareGPT¹ (Chiang et al., 2023). Following the data cleaning pipeline in (Zheng et al., 2023), we kept English conversations only, excluded those with less than 10,000 tokens, and split longer conversations so that we have a maximum sequence length of 16,384 tokens.

Evaluation Existing works primarily assess the efficacy of RoPE-extension methods through the examination of continual pre-trained models across language modeling tasks and synthetic tasks. For example, YaRN (Chen et al., 2023) evaluates the perplexity scores and model performance on the passkey-retrieval task (Mohtashami and Jaggi, 2023) to quantify models’ long-context performance. However, synthetic tasks like passkey retrieval deviate largely from real-world scenarios while language modeling tasks have also proved a rudimentary metric incapable of promising success in downstream tasks as suggested by Pal et al.

(2023); Sun et al. (2021). In this work, we analyzed the long context performance of models with extended context windows on selected tasks from LongBench (Bai et al., 2023). Our evaluation includes 12 tasks from four categories: single-document QA, multi-document QA, summarization, and few-shot learning to ensure a comprehensive evaluation of models’ long-context capabilities. We intentionally exclude synthetic tasks and code completion tasks from LongBench because synthetic tasks deviate largely from real-world scenarios, and code completion tasks have performance conflicts with general instruction following abilities learned from ShareGPT conversations, as suggested by Dong et al. (2023).

4.2 Measuring Long-Context Performance

To answer the research question “(1) Which method exhibits the best supervised fine-tuning performance on context-demanding downstream tasks?”, we fine-tune LLaMA-7B-Chat on 3.5k lengthy conversations and evaluate their long-context performance on LongBench.

Table 2 illustrates the performance of each method, with some results reported from the LongBench paper (Bai et al., 2023). We highlight our major observations here:

1) Fine-tuning the models on lengthy conversation data is efficient for context window extension. Both LongChat-v1.5-7B-32k and Vicuna-v1.5-7B-16k are open-source long-context models extended with PI (Chen et al., 2023) through fine-tuning on large amounts of conversation data. For example, LongChat-v1.5-7B-32 is finetuned on 80k conversations. By fine-tuning the model on lengthy conversations only, our replicated PI-based model outperformed the open-source versions, confirming the efficacy of fine-tuning the model on lengthy conversations.

2) PI yields better long-context fine-tuning results than YaRN. While NTK-By-Parts and YaRN have lower perplexity in language modeling tasks, PI has better fine-tuning performance on long-context downstream tasks that are more related to practical scenarios. This finding corroborates the conclusion by Pal et al. (2023); Sun et al. (2021) that language modeling perplexity is a rudimentary metric incapable of promising success in downstream tasks. We hypothesize that while YaRN’s scalar is efficient for language modeling tasks, its constant nature might affect model performance on downstream tasks.

¹<https://huggingface.co/datasets/philoschmid/sharegpt-raw>

Table 2: Experiment results on selected tasks from LongBench. Model names with a trailing asteroid are reported from the LongBench paper. We name our trained models after their RoPE-extension methods.

Model	Singl-Doc QA			Multi-Doc QA			Summarization			Few-shot Learning			Macro
	NQA	QAPR	MFQA_en	HPQA	WMQA	MSQ	GR	QMSM	MNWS	TREC	TRVQA	SMSM	
Llama2-7B-chat-4k*	18.7	19.2	36.8	25.4	32.8	9.4	27.3	20.8	25.8	61.5	77.8	40.7	33.0
LongChat-v1.5-7B-32k*	16.9	27.7	41.4	31.5	20.6	9.7	30.8	22.7	26.4	63.5	82.3	34.2	34.0
Vicuna-v1.5-7B-16k*	19.4	26.1	38.5	25.3	20.8	9.8	27.9	22.8	27.2	71.5	86.2	40.8	34.7
PI	20.1	30.4	45.3	26.1	30.1	9.9	28.1	23.7	26.6	68.0	84.9	42.5	36.3
NTK-By-Parts	15.9	31.1	40.1	25.4	26.6	7.2	26.7	22.4	26.9	68.5	82.8	42.9	34.7
Yarn	20.3	28.9	42.8	27.8	30.7	7.2	27.4	22.5	26.8	66.0	85.6	42.6	35.7
ABF	24.6	32.8	45.6	35.1	30.3	15.2	30.8	23.0	27.4	71.0	84.7	42.7	38.6
Ours	21.9	31.0	47.1	40.1	32.7	15.1	32.3	23.0	27.1	70.5	86.7	42.0	39.1

3) **ABF-based models surpass the other methods by a significant margin.** Both ABF and our methods exhibit consistently superior fine-tuning performance on all 12 long-context tasks, demonstrating the efficacy of adjusting RoPE’s base frequency to a large number (e.g. 50,000).

4.3 Measuring Data Efficiency

Data efficiency is an essential characteristic of RoPE-extension methods in context window extension practice, given both the sparsity of long training data and the high cost of training on long sequences. In this section, we explore the research question “(2) How can each method efficiently utilize training data?” by training the model respectively on 32, 100, 1k, and 3.5k conversations. The results are plotted in Figure 2, and the detailed results for each task are in Table 5.

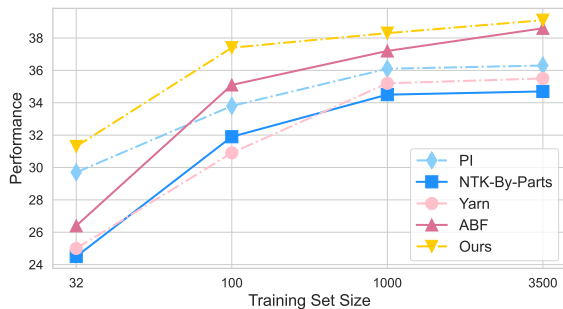


Figure 2: Long-Context Performance of RoPE-extending Methods with Different Amounts of Training Data

We highlight our major observations below:

1) **ABF-based methods consistently benefit from increasing training data.** While all RoPE-extension methods exhibit improved performance with increased training data, the performance gain appears marginal for PI, NTK-By-Parts, and Yarn when the data amount increases from 1K to 3.5K. Only ABF-based methods consistently demonstrate performance gains.

2) **Entropy-Aware ABF demonstrates extraordinary data efficiency.** Notably, with a mere **100** training samples and **6** training steps, our method achieves competitive long-context performance that only lags marginally behind the ABF method trained on 3.5K samples. Without considering the cost of finetuning on downstream tasks, PI (Chen et al., 2023) continue pre-trains LLaMA-7B (Touvron et al., 2023a) for 1,000 steps with 64 batch size, YaRN (Peng et al., 2023) adopts 250 continual pre-training steps with the same batch size. Open source practice like LongChat (Li* et al., 2023) utilizes 80k conversations from ShareGPT for instruction tuning. Our work demonstrates the remarkable efficiency of entropy-aware ABF in context window extension, requiring less than 2% of the training resources utilized by existing methodologies.

We also observe that the performance gap from ABF to our method is diminishing with the increase in training data. This phenomenon aligns with our hypothesis in Section 3.2 that while the ability to maintain concentration across lengthy inputs can be learned from training on more data, our method serves as an inductive bias that facilitates the learning process.

4.4 Measuring Robustness across Context Windows

A desirable attribute for RoPE-extension methods, when applied in practical context window extension settings, is that the models fine-tuned using these methods should maintain their performance on the original context window, while also demonstrating a certain degree of extrapolation capability beyond the fine-tuned length.

To answer the research question “(3) Do models trained with these methods have a robust performance across varying context window sizes?”, we follow LongBench (Bai et al., 2023) to assess the models across different context window sizes by truncating the prompt from the middle when the task length exceeds a designated context window

size.

The results are depicted in Figure 3. While there appears a performance gain for PI, NTK-By-Parts, and Yarn when the context size is enlarged from 4k to 8k, their performance degrades when the context is further enlarged to 16k, demonstrating their inability to leverage the full fine-tuning context window. In contrast, ABF and our proposed method consistently gain from a larger context window within fine-tuning length. Furthermore, entropy-aware ABF is the only method that can maintain the performance when directly extrapolating to 32k.

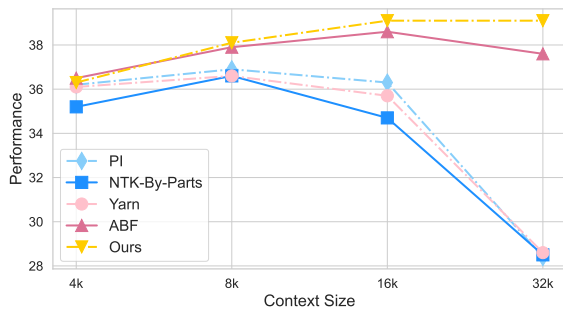


Figure 3: Long-Context Performance of RoPE-extending Methods with Different Context Window Sizes

4.5 Exploring the Optimal Training Data and Curriculums

In this section, we explore efficient training data and curriculums for context window extension on given tasks. An important consideration in practice is whether long in-domain training samples are indispensable for achieving success in context window extension for a particular downstream task. Specifically, we inquire whether short in-domain training samples only can still yield benefits in scenarios where lengthier samples are absent, which is often the case. To answer the above questions, we conduct experiments with various training curriculums on GovReport (Huang et al., 2021) which is a widely used long context summarization task, and Longchat-Line-Retrieval (Li* et al., 2023), a synthetic retrieval task.

We evaluate both long (more than 8,092 tokens) and short tasks (within 4,096 tokens) to guarantee models’ performance within the original context window while evaluating their long-context performance. When the training data is in-domain samples, we train the model for 4 epochs with a batch size of 8 and evaluate with the best epoch on

the validation set. When the training data is 1,000 ShareGPT conversations, the model is trained for two epochs with a batch size of 32 and evaluated on the second epoch.

The results are displayed in Table 3. We conclude that training the model on short in-domain samples produces suboptimal results, but starting from the model finetuned on 1,000 ShareGPT conversations yields comparable results to those finetuned on long in-domain samples, which suggests a good starting point for context window extension in practice.

It might be strange that the line-retrieval task shows extremely poor performance when finetuned from the Chat model on long samples. We attribute it to the insufficient training of our method because the answer to the line retrieval task is short, and we only calculate losses on the model response tokens during the instruction tuning.

Initialization	training data	GR-S	GR-L	LR-S	LR-L
LLaMA 2 Chat	None	30.84	0	76	0
LLaMA 2 Chat	Short	37.91	33.6	74	26
LLaMA 2 Chat	Long	38.24	36.45	10	2
Share1k	None	34.10	31.14	88	48
Share1k	Short	38.31	35.12	86	64
Share1k	Long	38.93	35.56	92	66
Short	Share1k	39.74	32.12	90	54

Table 3: Performance on two downstream tasks with different training curriculums. GR-S: GovReport-Short. GR-L: GovReport-Long. LR-S: Line Retrieval-Short. LR-L: LineRetrieval-Long. In the first column, **Share1k** means the fine-tuned result of the 7B Chat model on 1,000 ShareGPT conversations. **Short** means the fine-tuned result of the 7B chat model on short in-domain samples. In the second column, **None** means the model is directly tested. **Short** means short in-domain samples. **Long** means long in-domain samples.

5 Related Work

Extensive research has been done to enhance the long-context capacity of transformer models (Vaswani et al., 2017) by overcoming two prominent obstacles: the quadratic time and space complexity of the attention mechanism (Vaswani et al., 2017) and the inability of position encodings to generalize beyond the pre-trained context window.

More Efficient Transformers The vanilla attention mechanism in the Transformer architecture is known for its quadratic time and space complexity, which poses significant resource demands

for transformer models when processing lengthy inputs. Various works have focused on conquering the complexity issue and proposing more efficient Transformers. Sparse transformers (Child et al., 2019; Ye et al., 2019; Kitaev et al., 2020; Beltagy et al., 2020; Ainslie et al., 2020; Zaheer et al., 2020; Ding et al., 2023) replace the original full attention mechanism with a sparsified version to make the computation more efficient. Linear transformers (Wang et al., 2020; Katharopoulos et al., 2020; Choromanski et al., 2020), rather than forcing the attention mechanism to attend to fewer tokens, propose an alternative approach by leveraging low-rank matrix multiplication or linear dot-product of kernel feature maps to approximate the original attention mechanism, achieving linear time complexity. Meanwhile, retrieval-augmented models (Guu et al., 2020; Lewis et al., 2020; Wu et al., 2022; Bulatov et al., 2023; Tworkowski et al., 2023) integrate retrieval with attention. During inference time, these models avoid directly modeling lengthy inputs by retrieving information from an external memory that stores previous key-value pairs. While prior research primarily focuses on reducing FLOPs, the bottleneck of transformer inference on modern computing hardware has shifted to the overhead from memory access (IO). Multi-query attention (MQA)(Shazeer, 2019) and grouped-query attention (GQA)(Ainslie et al., 2023), for instance, address the memory-bandwidth cost associated with loading the large "keys" and "values" tensors in the multi-head attention mechanism by proposing the use of fewer "key" and "value" heads. Notably, GQA is employed in LLaMA2 (Touvron et al., 2023b). Additionally, FlashAttention (Dao et al., 2022; Dao, 2023) introduces an IO-aware exact attention approach that utilizes tiling to reduce memory IOs.

Generalizable Position Encoding Due to the attention mechanism’s parallel nature, transformer models require position encoding (PE) methods to facilitate the integration of position information. The original transformer employed sinusoidal position encoding, which constitutes an absolute PE and exhibits limited generalization capability. Subsequently, this approach was refined to a learnable version (Gehring et al., 2017), as embraced by language model architectures such as GPT-3 (Brown et al., 2020). However, this adaptation completely compromises the extrapolation ability of position encoding methods. The advent

of relative PE (Shaw et al., 2018) theoretically supports infinite input lengths. Nevertheless, despite recent advancements in relative PEs, such as T5 relative PE (Raffel et al., 2020), RoPE (Su et al., 2021), xPOS (Sun et al., 2022), and ALiBi (Press et al., 2021), it has been demonstrated by (Kazemnejad et al., 2023) that all these methods fail when extrapolating significantly beyond the pre-trained context window.

6 Conclusions

In summary, through interpreting LLMs’ inherent need to maintain concentration when processing lengthy sequences, we propose entropy-aware ABF by combining ABF with a sophisticated applied scalar that scales the attention logits. Our proposed method effectively extends the context window of RoPE-based LLMs, addressing their limitations when confronted with context-demanding tasks at a minimal cost. We empirically show the superiority of our method in both fine-tuning results and robustness across different context window sizes on various context-demanding tasks. Importantly, our method exhibits extraordinary data efficiency compared to other methods, deriving a competent long-context model on LongBench with only 100 samples and 6 training steps, less than 2% of the training resources utilized by previous works. Finally, we provide valuable insights into context window extension for specific downstream tasks, suggesting training on lengthy ShareGPT conversations as a good starting point.

7 Limitations

While we uncover that lengthy conversation data is efficient in finetuning LLMs for longer context windows, the availability and length distribution of such datasets are highly constrained. We leave for future work the development of more efficient and scalable training datasets for context window extension. Additionally, due to computational resource constraints, our investigation was restricted to the 7B parameter version of the LLaMA2 Chat model. Consequently, it remains an open question whether larger versions of LLaMA2, or other LLMs, exhibit similar characteristics to those observed in Figure 1, and therefore, whether they can also benefit from the methodology we have proposed.

References

- 675 Joshua Ainslie, James Lee-Thorp, Michiel de Jong, Yury
676 Zemlyanskiy, Federico Lebrón, and Sumit Sanghai.
677 2023. Gqa: Training generalized multi-query trans-
678 former models from multi-head checkpoints. *arXiv*
679 *preprint arXiv:2305.13245*.
- 680 Joshua Ainslie, Santiago Ontanon, Chris Alberti, Va-
681 clav Cvicek, Zachary Fisher, Philip Pham, Anirudh
682 Ravula, Sumit Sanghai, Qifan Wang, and Li Yang.
683 2020. Etc: Encoding long and structured inputs in
684 transformers. *arXiv preprint arXiv:2004.08483*.
- 685 Rohan Anil, Andrew M Dai, Orhan Firat, Melvin John-
686 son, Dmitry Lepikhin, Alexandre Passos, Siamak
687 Shakeri, Emanuel Taropa, Paige Bailey, Zhifeng
688 Chen, et al. 2023. Palm 2 technical report. *arXiv*
689 *preprint arXiv:2305.10403*.
- 690 Yushi Bai, Xin Lv, Jiajie Zhang, Hongchang Lyu,
691 Jiankai Tang, Zhidian Huang, Zhengxiao Du, Xiao
692 Liu, Aohan Zeng, Lei Hou, et al. 2023. Longbench:
693 A bilingual, multitask benchmark for long context
694 understanding. *arXiv preprint arXiv:2308.14508*.
- 695 Iz Beltagy, Matthew E Peters, and Arman Cohan. 2020.
696 Longformer: The long-document transformer. *arXiv*
697 *preprint arXiv:2004.05150*.
- 698 Sid Black, Stella Biderman, Eric Hallahan, Quentin
699 Anthony, Leo Gao, Laurence Golding, Horace He,
700 Connor Leahy, Kyle McDonell, Jason Phang, et al.
701 2022. Gpt-neox-20b: An open-source autoregressive
702 language model. *arXiv preprint arXiv:2204.06745*.
- 703 bloc97. 2023a. [Add NTK-Aware interpolation "by](#)
704 [parts" correction](#).
- 705 bloc97. 2023b. [NTK-Aware Scaled RoPE allows](#)
706 [LLaMA models to have extended \(8k+\) context size](#)
707 [without any fine-tuning and minimal perplexity degrada-](#)
708 [tion](#).
- 709 Tom Brown, Benjamin Mann, Nick Ryder, Melanie
710 Subbiah, Jared D Kaplan, Prafulla Dhariwal, Arvind
711 Neelakantan, Pranav Shyam, Girish Sastry, Amanda
712 Askell, et al. 2020. Language models are few-shot
713 learners. *Advances in neural information processing*
714 *systems*, 33:1877–1901.
- 715 Aydar Bulatov, Yuri Kuratov, and Mikhail S Burtsev.
716 2023. Scaling transformer to 1m tokens and beyond
717 with rmt. *arXiv preprint arXiv:2304.11062*.
- 718 Shouyuan Chen, Sherman Wong, Liangjian Chen, and
719 Yuandong Tian. 2023. Extending context window of
720 large language models via positional interpolation.
721 *arXiv preprint arXiv:2306.15595*.
- 722 Tianqi Chen, Bing Xu, Chiyuan Zhang, and Carlos
723 Guestrin. 2016. Training deep nets with sublinear
724 memory cost. *arXiv preprint arXiv:1604.06174*.
- 725 David Chiang and Peter Cholak. 2022. Overcoming a
726 theoretical limitation of self-attention. *arXiv preprint*
727 *arXiv:2202.12172*.
- Wei-Lin Chiang, Zhuohan Li, Zi Lin, Ying Sheng,
Zhanghao Wu, Hao Zhang, Lianmin Zheng, Siyuan
Zhuang, Yonghao Zhuang, Joseph E. Gonzalez, Ion
Stoica, and Eric P. Xing. 2023. Vicuna: An open-
source chatbot impressing gpt-4 with 90%* chatgpt
quality.
- Rewon Child, Scott Gray, Alec Radford, and
Ilya Sutskever. 2019. Generating long se-
quences with sparse transformers. *arXiv preprint*
arXiv:1904.10509.
- Krzysztof Choromanski, Valerii Likhoshesterov, David
Dohan, Xingyou Song, Andreea Gane, Tamas Sar-
los, Peter Hawkins, Jared Davis, Afroz Mohiuddin,
Lukasz Kaiser, et al. 2020. Rethinking attention with
performers. *arXiv preprint arXiv:2009.14794*.
- Aakanksha Chowdhery, Sharan Narang, Jacob Devlin,
Maarten Bosma, Gaurav Mishra, Adam Roberts, Paul
Barham, Hyung Won Chung, Charles Sutton, Sebas-
tian Gehrmann, et al. 2023. Palm: Scaling language
modeling with pathways. *Journal of Machine Learn-*
ing Research, 24(240):1–113.
- Tri Dao. 2023. Flashattention-2: Faster attention with
better parallelism and work partitioning. *arXiv*
preprint arXiv:2307.08691.
- Tri Dao, Dan Fu, Stefano Ermon, Atri Rudra, and
Christopher Ré. 2022. Flashattention: Fast and
memory-efficient exact attention with io-awareness.
Advances in Neural Information Processing Systems,
35:16344–16359.
- Jiayu Ding, Shuming Ma, Li Dong, Xingxing Zhang,
Shaohan Huang, Wenhui Wang, and Furu Wei. 2023.
Longnet: Scaling transformers to 1,000,000,000 to-
kens. *arXiv preprint arXiv:2307.02486*.
- Guanting Dong, Hongyi Yuan, Keming Lu, Cheng-
peng Li, Mingfeng Xue, Dayiheng Liu, Wei Wang,
Zheng Yuan, Chang Zhou, and Jingren Zhou. 2023.
How abilities in large language models are affected
by supervised fine-tuning data composition. *arXiv*
preprint arXiv:2310.05492.
- Leo Gao, Stella Biderman, Sid Black, Laurence Gold-
ing, Travis Hoppe, Charles Foster, Jason Phang, Ho-
race He, Anish Thite, Noa Nabeshima, et al. 2020.
The pile: An 800gb dataset of diverse text for lan-
guage modeling. *arXiv preprint arXiv:2101.00027*.
- Jonas Gehring, Michael Auli, David Grangier, Denis
Yarats, and Yann N Dauphin. 2017. Convolutional se-
quence to sequence learning. In *International confer-*
ence on machine learning, pages 1243–1252. PMLR.
- Kelvin Guu, Kenton Lee, Zora Tung, Panupong Pasu-
pat, and Mingwei Chang. 2020. Retrieval augmented
language model pre-training. In *International confer-*
ence on machine learning, pages 3929–3938. PMLR.
- Luyang Huang, Shuyang Cao, Nikolaus Parulian, Heng
Ji, and Lu Wang. 2021. Efficient attentions for
long document summarization. *arXiv preprint*
arXiv:2104.02112.

784	kaiokendev. 2023. Things I'm learning while training superhot .	837
785		838
786	Angelos Katharopoulos, Apoorv Vyas, Nikolaos Pappas, and François Fleuret. 2020. Transformers are rnns: Fast autoregressive transformers with linear attention. In <i>International conference on machine learning</i> , pages 5156–5165. PMLR.	839
787		840
788		841
789		842
790		
791	Amirhossein Kazemnejad, Inkit Padhi, Karthikeyan Natesan Ramamurthy, Payel Das, and Siva Reddy. 2023. The impact of positional encoding on length generalization in transformers. <i>arXiv preprint arXiv:2305.19466</i> .	843
792		844
793		845
794		846
795		847
796	Nikita Kitaev, Łukasz Kaiser, and Anselm Levskaya. 2020. Reformer: The efficient transformer. <i>arXiv preprint arXiv:2001.04451</i> .	848
797		849
798		850
799	Patrick Lewis, Ethan Perez, Aleksandra Piktus, Fabio Petroni, Vladimir Karpukhin, Naman Goyal, Heinrich Küttler, Mike Lewis, Wen-tau Yih, Tim Rocktäschel, et al. 2020. Retrieval-augmented generation for knowledge-intensive nlp tasks. <i>Advances in Neural Information Processing Systems</i> , 33:9459–9474.	851
800		852
801		853
802		854
803		855
804		856
805	Dacheng Li*, Rulin Shao*, Anze Xie, Ying Sheng, Lianmin Zheng, Joseph E. Gonzalez, Ion Stoica, Xuezhe Ma, and Hao Zhang. 2023. How long can open-source llms truly promise on context length?	857
806		858
807		859
808		860
809	Tianyang Liu, Canwen Xu, and Julian McAuley. 2023. Repobench: Benchmarking repository-level code auto-completion systems. <i>arXiv preprint arXiv:2306.03091</i> .	861
810		862
811		863
812		864
813	Ilya Loshchilov and Frank Hutter. 2017. Decoupled weight decay regularization. <i>Learning, Learning</i> .	865
814		866
815	Amirkeivan Mohtashami and Martin Jaggi. 2023. Landmark attention: Random-access infinite context length for transformers. <i>arXiv preprint arXiv:2305.16300</i> .	867
816		868
817		869
818		870
819	Arka Pal, Deep Karkhanis, Manley Roberts, Samuel Dooley, Arvind Sundararajan, and Siddhartha Naidu. 2023. Giraffe: Adventures in expanding context lengths in llms. <i>arXiv preprint arXiv:2308.10882</i> .	871
820		872
821		873
822		874
823	Bowen Peng, Jeffrey Quesnelle, Honglu Fan, and Enrico Shippole. 2023. Yarn: Efficient context window extension of large language models. <i>arXiv preprint arXiv:2309.00071</i> .	875
824		876
825		877
826		878
827	Ofir Press, Noah A Smith, and Mike Lewis. 2021. Train short, test long: Attention with linear biases enables input length extrapolation. <i>arXiv preprint arXiv:2108.12409</i> .	879
828		880
829		881
830		882
831	Colin Raffel, Noam Shazeer, Adam Roberts, Katherine Lee, Sharan Narang, Michael Matena, Yanqi Zhou, Wei Li, and Peter J Liu. 2020. Exploring the limits of transfer learning with a unified text-to-text transformer. <i>The Journal of Machine Learning Research</i> , 21(1):5485–5551.	883
832		884
833		885
834		886
835		887
836		888
		889
		890
		891
		892
		893
		894
		895
		896
		897
		898
		899
		900
		901
		902
		903
		904
		905
		906
		907
		908
		909
		910
		911
		912
		913
		914
		915
		916
		917
		918
		919
		920
		921
		922
		923
		924
		925
		926
		927
		928
		929
		930
		931
		932
		933
		934
		935
		936
		937
		938
		939
		940
		941
		942
		943
		944
		945
		946
		947
		948
		949
		950
		951
		952
		953
		954
		955
		956
		957
		958
		959
		960
		961
		962
		963
		964
		965
		966
		967
		968
		969
		970
		971
		972
		973
		974
		975
		976
		977
		978
		979
		980
		981
		982
		983
		984
		985
		986
		987
		988
		989
		990
		991
		992
		993
		994
		995
		996
		997
		998
		999
		1000

- 893 Ashish Vaswani, Noam Shazeer, Niki Parmar, Jakob
894 Uszkoreit, Llion Jones, Aidan N Gomez, Łukasz
895 Kaiser, and Illia Polosukhin. 2017. Attention is all
896 you need. *Advances in neural information processing*
897 *systems*, 30.
- 898 Sinong Wang, Belinda Z Li, Madian Khabsa, Han Fang,
899 and Hao Ma. 2020. Linformer: Self-attention with
900 linear complexity. *arXiv preprint arXiv:2006.04768*.
- 901 Yuhuai Wu, Markus N Rabe, DeLesley Hutchins, and
902 Christian Szegedy. 2022. Memorizing transformers.
903 *arXiv preprint arXiv:2203.08913*.
- 904 Wenhan Xiong, Jingyu Liu, Igor Molybog, Hejia Zhang,
905 Prajjwal Bhargava, Rui Hou, Louis Martin, Rashi
906 Rungta, Karthik Abinav Sankararaman, Barlas Oguz,
907 et al. 2023. Effective long-context scaling of founda-
908 tion models. *arXiv preprint arXiv:2309.16039*.
- 909 Zihao Ye, Qipeng Guo, Quan Gan, Xipeng Qiu, and
910 Zheng Zhang. 2019. Bp-transformer: Modelling
911 long-range context via binary partitioning. *arXiv:*
912 *Computation and Language, arXiv: Computation and*
913 *Language*.
- 914 Manzil Zaheer, Guru Guruganesh, Kumar Avinava
915 Dubey, Joshua Ainslie, Chris Alberti, Santiago On-
916 tanon, Philip Pham, Anirudh Ravula, Qifan Wang,
917 Li Yang, et al. 2020. Big bird: Transformers for
918 longer sequences. *Advances in neural information*
919 *processing systems*, 33:17283–17297.
- 920 Lianmin Zheng, Wei-Lin Chiang, Ying Sheng, Siyuan
921 Zhuang, Zhonghao Wu, Yonghao Zhuang, Zi Lin,
922 Zhuohan Li, Dacheng Li, Eric P Xing, Hao Zhang,
923 Joseph E. Gonzalez, and Ion Stoica. 2023. [Judging](#)
924 [llm-as-a-judge with mt-bench and chatbot arena](#).

925 A Training Details

926 The model is trained on 4 NVIDIA A100 GPUs
927 with DeepSpeed (Rasley et al., 2020), ZeRO (Ra-
928 jbandari et al., 2020; Ren et al., 2021) Stage 3,
929 gradient-checkpointing (Chen et al., 2016), and
930 FlashAttention (Dao et al., 2022; Dao, 2023). We
931 also use BF16 and TF32 mix computation precision
932 for further acceleration.

933 All the models are fine-tuned using AdamW
934 Optimizer (Loshchilov and Hutter, 2017) with
935 $\beta_1 = 0.9$ and $\beta_2 = 0.95$ for two epochs, com-
936 puting losses on response tokens only. We use a
937 cosine learning rate scheduler, set the peak learning
938 rate to $2e-5$, and weight decay to 0.1. For training
939 on 3.5k conversations, we use a batch size of 128
940 and 10 warmup steps. We use a batch size of 32 and
941 0 warmup steps for fewer training data. If not ex-
942 plicitly stated, we default to using 3.5k ShareGPT
943 conversations for instruction tuning.

944 B Additional Experiment Results

Model	Singl-Doc QA			Multi-Doc QA			Summarization			Few-shot Learning			Macro
	NQA	QAPR	MFQA_en	HPQA	WMQA	MSQ	GR	QMSM	MNWS	TREC	TRVQA	SMSM	
PI-4K	22.3	27.3	44.6	31.7	30.8	9.2	29.3	21.5	27.1	61.5	87.5	41.4	36.2
PI-8K	21.4	28.6	46.8	31.1	29	11.7	30.1	22.5	27.1	66	86.8	42.2	36.9
PI-16K	20.1	30.4	45.3	26.1	30.1	9.9	28.1	23.7	26.6	68	84.9	42.5	36.3
PI-32K	7	27.6	43.7	16.3	25.1	1.5	23.5	14.2	27	67.5	54.4	33.1	28.4
NTK-By-Parts-4k	22.8	27.3	42.5	26.5	23	10.1	28.7	21.8	27.1	63	87.3	42	35.2
NTK-By-Parts-8k	20.9	31.2	43.5	28.3	29.4	10.9	29.4	22.3	27	65	87.5	43.5	36.6
NTK-By-Parts-16k	15.9	31.1	40.1	25.4	26.6	7.2	26.7	22.4	26.9	68.5	82.8	42.9	34.7
NTK-By-Parts-32k	6.5	30.8	39.1	15.9	26.2	1.1	23.3	14.9	26.9	68.5	54.4	34.7	28.5
Yarn-4K	21	27.9	43.8	29	29.5	12.8	29.3	22.1	26.9	61.5	87.1	42.8	36.1
Yarn-8K	20.9	31.2	43.5	28.3	29.4	10.9	29.4	22.3	27	65	87.5	43.5	36.6
Yarn-16K	20.3	28.9	42.8	27.8	30.7	7.2	27.4	22.5	26.8	66	85.6	42.6	35.7
Yarn-32K	6.5	29.3	39	16	29.1	1.3	24	14.4	26.9	66.5	55.1	34.6	28.6
ABF-4K	19.5	30.6	44.1	31.1	29.5	11.5	29	21.4	27.6	64.5	87.6	41.9	36.5
ABF-8K	22.7	32.1	45.2	35.5	29.2	14.8	30.6	22.8	27.4	67	84.8	42.4	37.9
ABF-16K	24.6	32.8	45.6	35.1	30.3	15.2	30.8	23	27.4	71	84.7	42.7	38.6
ABF-32K	23.6	27.1	44.8	36.8	27.5	12.3	29.4	23.1	26.5	72	84.9	43.5	37.6
Ours-4K	21.1	30.1	43.3	28.1	31.6	11.1	28.7	21.6	27.6	64	86.8	42.1	36.3
Ours-8K	23.3	31.7	45.5	33.2	31.7	14.6	30.7	23	27	67.5	86.3	42.4	38.1
Ours-16K	21.9	31	47.1	40.1	32.7	15.1	32.3	23	27.1	70.5	86.7	42	39.1
Ours-32K	23.6	31.8	45.5	39	31.7	16.6	31.7	23.6	27.1	70.5	86	42.4	39.1

Table 4: Long-Context performance of RoPE-extension Methods with different context window sizes

Model	Singl-Doc QA			Multi-Doc QA			Summarization			Few-shot Learning			Macro
	NQA	QAPR	MFQA_en	HPQA	WMQA	MSQ	GR	QMSM	MNWS	TREC	TRVQA	SMSM	
PI-32	10.7	15.2	30.5	18.5	21.6	7.3	31	21.2	27.5	60	73.2	39.4	29.7
PI-100	7.2	31.4	37.1	30.9	33.4	11.6	30.5	16	27.1	64.5	78.4	38	33.8
PI-1000	20.4	31.1	39	30.7	30.5	10.4	27.9	23.5	26.6	67	84.5	41.6	36.1
PI-3500	20.1	30.4	45.3	26.1	30.1	9.9	28.1	23.7	26.6	68	84.9	42.5	36.3
NTK-By-Parts-32	4.5	22.6	31.9	10.9	23.7	0.8	20.7	13.2	26.3	65	41.3	33.4	24.5
NTK-By-Parts-100	7.9	28.6	40.1	19.1	26.9	7	24.7	18	26.1	66.5	77.3	40	31.9
NTK-By-Parts-1000	15.9	28.3	42.7	23.6	26.5	6.5	26.4	22.7	26.7	68.5	83.7	42.1	34.5
NTK-By-Parts-3500	15.9	31.1	40.1	25.4	26.6	7.2	26.7	22.4	26.9	68.5	82.8	42.9	34.7
Yarn-32	5	18.9	35.1	12	26	0.9	23.6	14.1	26.2	63.5	44.1	30.4	25
Yarn-100	6.6	30.1	39.2	17.7	27.1	2.8	24.4	16.7	25.8	66.5	76	37.9	30.9
Yarn-1000	18	28.2	42.9	26.7	28.4	9.3	27.6	22.4	26.9	65	85.1	41.9	35.2
Yarn-3500	19.7	25.4	44.6	29.3	25.9	9.5	26.5	22.2	26.7	67.5	85.6	43.7	35.5
ABF-32	10.9	15	32.2	20.3	21.6	7.5	28.3	21.2	26.9	56	41.6	35.2	26.4
ABF-100	18.8	27.6	41.2	30.9	35	10.2	31.3	22	27.2	66.5	73.8	36.7	35.1
ABF-1000	23.9	33	44.9	32	20.1	12.2	31.1	23.9	27.5	71	85.6	40.7	37.2
ABF-3500	24	30.5	45.8	37.9	30.7	15.4	31.4	23.3	27.2	70	84.2	42.6	38.6
Ours-32	14.8	15.6	36.4	29.6	25.9	12.9	32.2	21.4	26.9	55	67.3	38.1	31.3
Ours-100	20.6	26.4	45.9	37.7	35.6	16.4	32.2	22	26.9	67.5	80.2	37.3	37.4
Ours-1000	23.5	33	45	34.3	24.8	16.4	30.9	23.8	27.9	71	87.7	41	38.3
Ours-3500	21.9	31	47.1	40.1	32.7	15.1	32.3	23	27.1	70.5	86.7	42	39.1

Table 5: Long-context performance of RoPE-extension methods with different amounts of training data